Geophysical Research Letters

RESEARCH LETTER
10.1029/2023GL105130

A North–South Dipole Response of the South Atlantic Convergence Zone During the Mid-Holocene

Minn Lin Wong[1,2], David S. Battisti[3], Xiaojuan Liu[4], Qinghua Ding[5], and Xianfeng Wang[1,2]

[1]Asian School of the Environment, Nanyang Technological University, Singapore, Singapore, [2]Earth Observatory of Singapore, Nanyang Technological University, Singapore, Singapore, [3]Department of Atmospheric Sciences, University of Washington, Seattle, WA, USA, [4]Deptarment of Earth and Planetary Science, University of California, Berkeley, Berkeley, CA, USA, [5]Department of Geography & ERI, University of California, Santa Barbara, Santa Barbara, CA, USA

Key Points:

- Model experiments show a north–south dipole response of the South Atlantic Convergence Zone during the mid-Holocene
- The dipole response in precipitation is consistent with the mid-Holocene hydroclimate changes observed in proxy records
- The dipole response is linked to the strength of the South Atlantic subtropical high and the South American low-level Jet

Supporting Information:

Supporting Information may be found in the online version of this article.

Correspondence to:

M. L. Wong,
minnlin001@e.ntu.edu.sg

Citation:

Wong, M. L., Battisti, D. S., Liu, X., Ding, Q., & Wang, X. (2023). A north–south dipole response of the South Atlantic Convergence Zone during the mid-Holocene. *Geophysical Research Letters*, *50*, e2023GL105130. https://doi.org/10.1029/2023GL105130

Received 27 JUN 2023
Accepted 18 OCT 2023

Author Contributions:

Conceptualization: Minn Lin Wong, David S. Battisti
Funding acquisition: Minn Lin Wong
Investigation: Minn Lin Wong
Methodology: Minn Lin Wong
Resources: David S. Battisti, Xiaojuan Liu, Qinghua Ding
Supervision: Xianfeng Wang
Writing – original draft: Minn Lin Wong
Writing – review & editing: David S. Battisti, Xiaojuan Liu, Qinghua Ding, Xianfeng Wang

Abstract The South Atlantic Convergence Zone (SACZ) profoundly modulates precipitation from central to southeastern Brazil in the present-day climate. However, the understanding of its long-term behavior responding to various climate forcings remains limited. Here, we use an isotope-enabled atmospheric general circulation model (ECHAM4.6) to examine the precipitation response of the SACZ during the mid-Holocene about six thousand years ago. The model simulates a northward intensification of the SACZ in the mid-Holocene, resulting in a dipole anomaly pattern relative to today's climate. The mid-Holocene precipitation increased along the northern margin of the SACZ due to the strengthening of easterly winds across the tropical Atlantic, while an eastward deflection of the South American low-level jet reduced moisture transport to southern Brazil, resulting in reduced precipitation along the southern margins of the SACZ. The north–south dipole response in precipitation is consistent with the mid-Holocene hydroclimate change observed in proxy records from the region.

Plain Language Summary The South Atlantic Convergence Zone (SACZ) is a key climatic feature of the South American Summer Monsoon (SASM) season and bears significant importance to the South American population. Understanding the long-term behavior of the convergence zone is therefore vital for predicting future change in rainfall patterns across eastern South America. Using terrestrial climate records and atmospheric general circulation model experiments, we investigated SACZ precipitation over the past 7,000 years. Our findings reveal that rainfall anomalies in northeastern and southern Brazil exhibited a see-saw pattern, while the peak rainfall position over central Brazil remained constant. We show that rainfall along the margins of the SACZ is particularly sensitive to the strength of the SASM. This study therefore holds important implications for water resource management in tropical South America in the face of projected future changes in the SASM.

1. Introduction

1.1. The Modern-Day Precipitation in Tropical South America

The eastern region of South America hosts a wide range of ecoregions, from the humid evergreen tropical forests in the eastern Amazon to the arid Cerrado and Caatinga biome in central and northeastern Brazil (Smith & Mayle, 2018). Sharp transitions in the ecology are a result of several interacting climate features that contribute to the complex hydrology of eastern South America. In addition to the South American Summer Monsoon (SASM) and the Intertropical Convergence Zone (ITCZ), the South Atlantic Convergence Zone (SACZ) also influences precipitation patterns over eastern tropical to subtropical South America.

The SACZ is a region of enhanced convection during the austral summer months (December to February [DJF]) that extends diagonally (northwest to southeast) across central South America (Figure 1a). The SACZ is a result of the convergence between the northerly inflow from the western periphery of the South Atlantic Subtropical High (SASH) over the Atlantic Ocean, and the westerly inflow from the Amazon driven by the Chaco Low (CL) (Kodama, 1993) (Figure 1b). At intra-seasonal timescales, the SACZ is forced by propagating transient and quasi-stationary Rossby waves from the mid-latitudes, but its overall mean position is predominantly controlled by large-scale flow from Amazon convection (Liebmann et al., 2004). Therefore, the climatological position of the SACZ is closely associated with the direction and intensity of the low-level jet (LLJ) that transports moisture

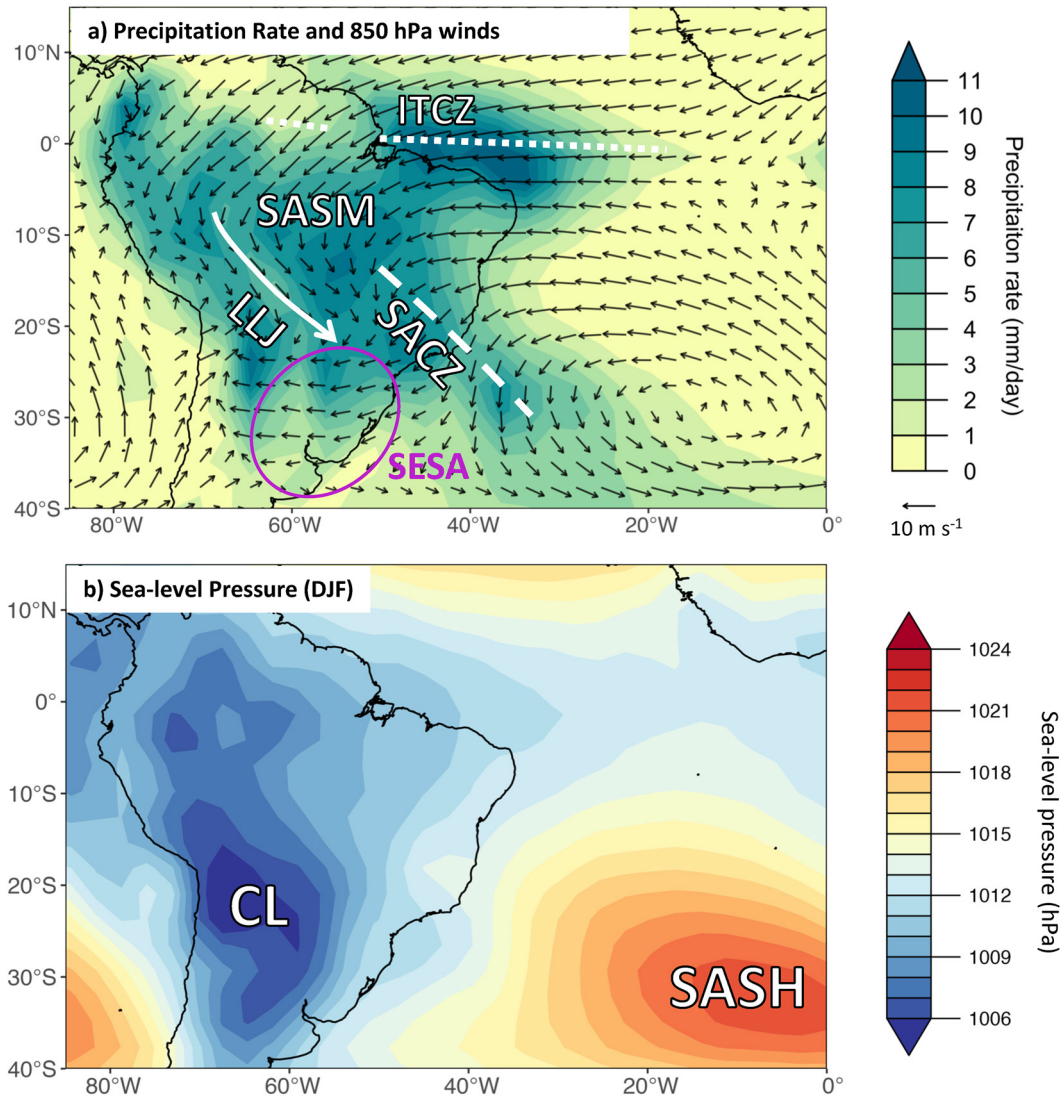

Figure 1. Map of austral summer (December to February [DJF]) modern-day precipitation climatology over South America simulated by the ECHAM4.6–slab ocean. (a) Shading represents the average DJF precipitation. Climate features of the South American Summer Monsoon system are highlighted by the white text for the low-level jet (white arrow), South Atlantic Convergence Zone axis (dashed line) and the Intertropical Convergence Zone (stippled line). The southeastern South America region is highlighted by the purple oval. (b) Averaged sea-level pressure in DJF, showing the Chaco Low over the continent and the South Atlantic Subtropical High over the ocean.

from the Amazon to southeastern South America (SESA), encompassing southern Brazil, Uruguay, parts of Paraguay, and northern Argentina (Figure 1a) (Boers et al., 2014; Zilli et al., 2019).

The present-day variability of the SACZ is associated with latitudinal shifts from its typical position represented by the climatological mean maximum in SACZ precipitation. These latitudinal shifts can modulate rainfall in a north-south pattern between central Brazil and SESA. For instance, the latitudinal migration toward the north or south can either inhibit or support precipitation anomalies in the SESA region (Nielsen et al., 2019), resulting in anti-phased precipitation anomalies flanking the typical SACZ core region over central Brazil and SESA. Observations have shown that the SACZ undergoes migrations at various timescales ranging from intraseasonal to decadal, with these shifts being attributed to factors such as tropical Atlantic sea surface temperature (SST) variability (Jorgetti et al., 2013; Robertson & Mechoso, 2000; Zilli et al., 2019) and the El Niño-Southern Oscillation (Carvalho et al., 2004; De Souza & Ambrizzi, 2006). While modern-day instrumental records suggest that the SACZ can undergo latitudinal shifts in its position, the long-term change in the SACZ due to natural (e.g., Orbital) and anthropogenic forcings are less well understood.

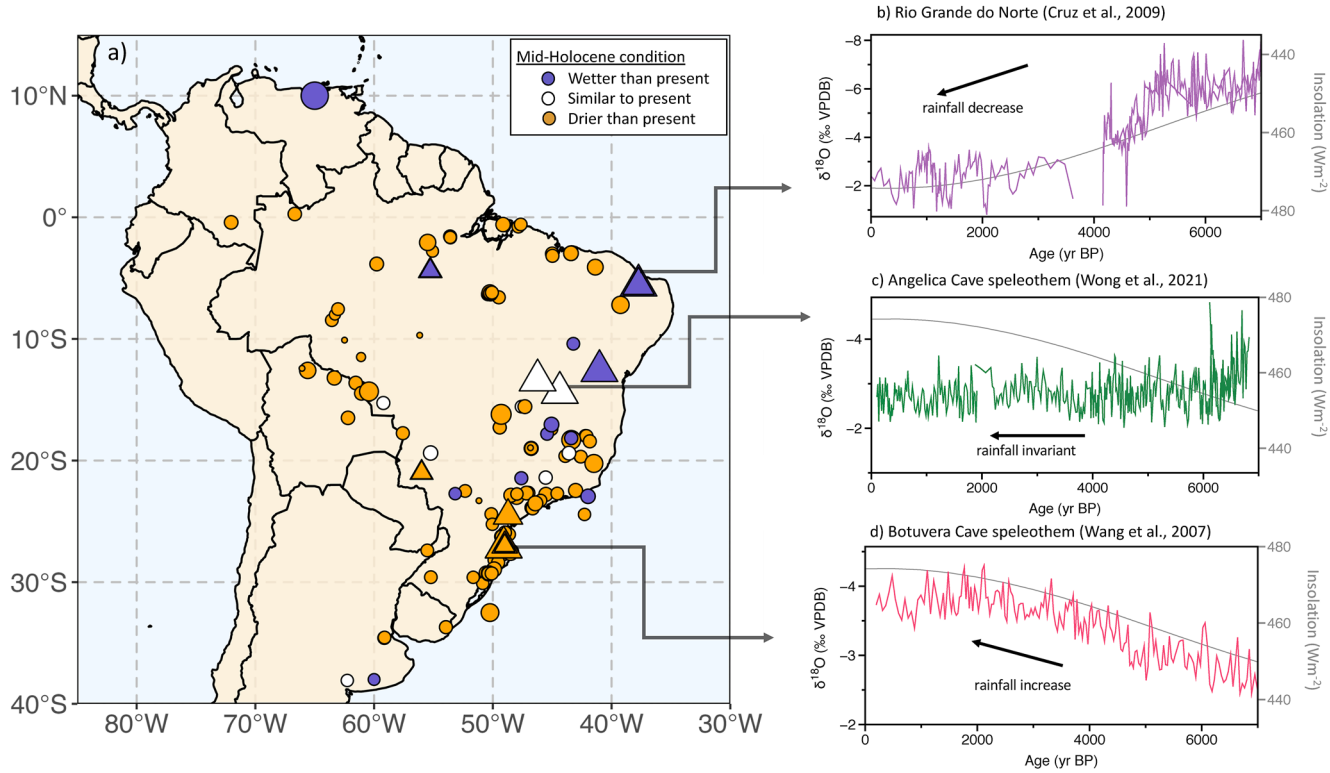

Figure 2. Hydroclimate proxy records across tropical South America that indicate mid-Holocene conditions. (a) Map of hydroclimate records and the interpreted mid-Holocene conditions where a wetter, similar, or drier condition is indicated by the purple, white, and orange colors, respectively. The size of the symbols represent the quality of the records based on Gorenstein et al. (2022). Circles are sediment and soil records while triangles are speleothem records. See Table S2 in Supporting Information S1 for individual references. (b) The Rio Grande Norte speleothem $\delta^{18}O$ record from northeastern Brazil (Cruz et al., 2009). (c) The Angelica Cave speleothem $\delta^{18}O$ record from central Brazil (Wong et al., 2021a). (d) Botuvera Cave speleothem $\delta^{18}O$ record from southern Brazil (X. Wang et al., 2007). The gray curve in panels (b–d) represents January insolation values at 15°S (Laskar et al., 2004).

1.2. Precipitation Change During the Mid-Holocene

The mid-Holocene, defined by the Paleoclimate Modelling Intercomparison Project Phase 4 (PMIP4) as the time period around 6 thousand years ago before present (kyr BP) (Otto-Bliesner et al., 2017), is particularly appropriate for studying long-term climate change because there are numerous, well-dated proxy records of the hydroclimate of South America and of the large, orbitally induced changes in insolation, while the continental geometry, orography and greenhouse gas concentrations are very similar to that in the pre-industrial period.

Paleo-hydroclimate proxy records along the eastern region of South America often show contrasting signals across latitudes during the mid-Holocene (Figure 2). Broadly, there is a north–south anti-phased pattern in precipitation trends. Along coastal northeastern Brazil, speleothem records indicate wetter mid-Holocene conditions compared to the modern-day, as evidenced by an increasing $\delta^{18}O$ trend from the mid-Holocene to the pre-industrial (Figure 2b). Several hypotheses have been put forward to explain these observations, including a southward migration of the ITCZ (Chiessi et al., 2021), a weakened SASM and correspondingly reduced subsidence in the northeast due to a weaker Nordeste Low (Cruz et al., 2009), or teleconnections with the African continent (Cook et al., 2004; Liu & Battisti, 2015).

Further south, in the vicinity of the SACZ, several speleothem and pollen records from central to central-eastern Brazil instead show similar mid-Holocene moisture conditions as the modern-day, suggesting little-to-no change in precipitation near the SACZ axis (Figure 2c) (Strikis et al., 2011; Wong et al., 2021b). Over SESA, the majority of hydroclimate records show drier mid-Holocene conditions (e.g., Figure 2c). Drier conditions over SESA could be a result of a weaker transport of moisture from the Amazon to the subtropics by the LLJ (X. Wang et al., 2007). However, some studies propose that the SACZ may have migrated latitudinally southwards toward the late-Holocene to its present position over SESA (Bernal et al., 2016; Perez Filho et al., 2022; X. Wang

et al., 2006), which has been used to explain drier mid-Holocene conditions in southern Brazil compared to today. However, there has yet to be a close examination of the SACZ response to orbital-scale insolation forcing.

In this study, we investigate how the SACZ responded to the insolation changes over the mid-to-late Holocene by employing an isotope-enabled atmospheric general circulation model (AGCM) coupled to a slab ocean model (ECHAM4.6–slab ocean) in order to simulate the precipitation change between the mid-Holocene and pre-industrial period. We conduct a transect analysis across the SACZ to evaluate how the SACZ responded to mid-Holocene forcings and its contribution to changes in regional rainfall. These isotope-enabled experiments will allow us to directly compare the model result with proxy data in the region and thus provide insight into the sensitivity of local precipitation to various climate factors. This comparison will also serve as a testbed to better understand the capability of our climate models in representing climate responses over the region to different levels of orbital forcing. Thus, the finding of this research has direct implications for both paleo and modern climate communities.

2. Methods

2.1. Model Simulations

The AGCM used in this study is the ECHAM4.6 developed at the Max Planck Institute for Meteorology. The ECHAM4.6 model was run with a spectral T42 resolution (approximately 2.78° lat. × 2.78° long.) with 19 vertical levels of atmosphere (Roeckner et al., 1996). Although the newer version of this model, ECHAM6, has a higher resolution at T64 (approximately 1.876° lat. × 1.876° long.), we favor version 4.6 which already has a sufficient spatial resolution to investigate large-scale precipitation patterns such as the SACZ. Importantly, the ECHAM4.6 is equipped with a module that allows us to simulate the evolution of water isotopes that can be compared to the $\delta^{18}O$ records in the region (Hoffmann et al., 1998). To simulate thermodynamic ocean feedback, the ECHAM4.6 atmospheric component is coupled to a 50 m slab ocean model. We additionally prescribe a cyclostationary heat flux (known as the "q-flux") to account for the seasonal cycle of heat input to the atmosphere caused by oceanic circulation (Battisti et al., 2014). Hence, change in ocean heat transport convergence are not accounted for in the model.

To investigate mid-Holocene precipitation change, we simulate the mid-Holocene and pre-industrial climate. Differences in physical parameters between these two time periods mainly lie in the changes in orbital configuration which result in differences in the distribution of solar radiation at the Earth's top of atmosphere. Specific values for the orbital parameters and trace gas concentrations used are shown in Table S1 in Supporting Information S1 and follow the experimental design protocol for the PMIP4/CMIP6 simulations described in Otto-Bliesner et al. (2017).

The pre-industrial scenario refers to the climate before the 1850s, prior to significant anthropogenic influence; therefore, CO_2 is set at 284.3 ppmv. The orbital parameters are very similar to modern-day values. Compared to the pre-industrial period, the mid-Holocene received significantly lower Southern Hemisphere summer insolation–about 30 W/m^2 less at 10°S (Laskar et al., 2004). For the mid-Holocene and pre-industrial scenarios, each experiment was run for 41 years. The first year of the model run is discarded to avoid any problems with equilibration during the model spin-up. Since the model is equipped with a slab ocean model, we believe that our simulation doesn't require a long spin-up which is normally needed for a fully coupled model. In the 40-year simulation, the mean state of most climate fields (e.g., rainfall, wind circulation, etc.) in the first half is very similar to those in the second half, indicating that the simulation operates under an equilibrium state throughout the whole integration period.

One limitation of this modeling approach is that the full feedback of deeper ocean dynamics may not be well reflected by the slab ocean model. On the other hand, by incorporating a slab ocean and the q-flux correction step, our model minimizes biases associated with a full ocean model, such as the double ITCZ bias (Samanta et al., 2019) and SST biases over the Southern Ocean (C. Wang et al., 2014).

2.2. Hydroclimate Proxies

The model results are compared to a compilation of existing hydroclimate proxies, based on the compilation by Gorenstein et al. (2022) and Prado et al. (2013) that consist of sediment, soil and speleothem records spanning the mid-to-late Holocene. Each of the records indicates either a wetter, drier, or similar-to-present mid-Holocene climate and includes a quality index based on sampling resolution and the number of dates within

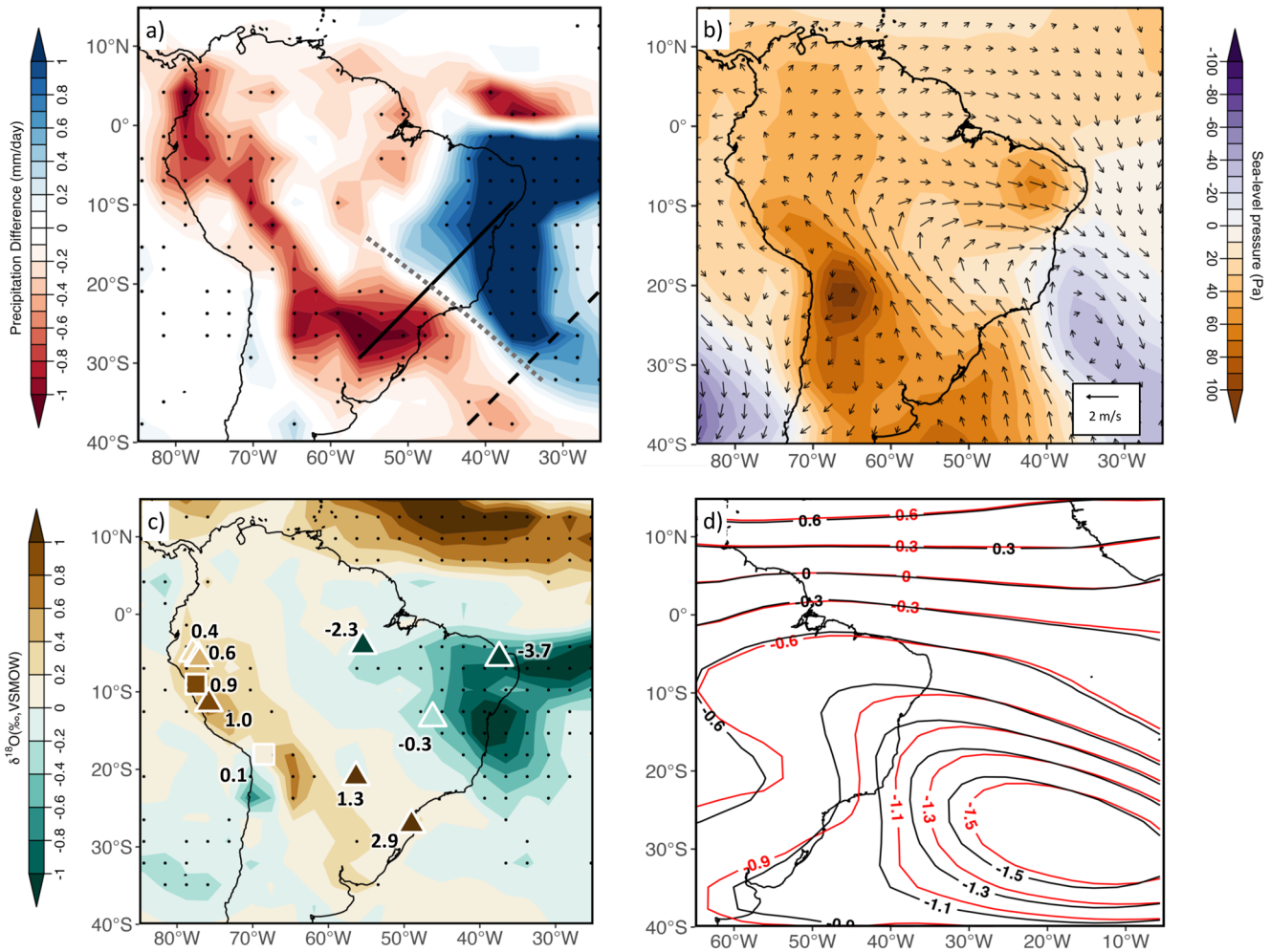

Figure 3. Comparisons between the mid-Holocene and pre-industrial scenarios simulated by the ECHAM4.6–slab ocean model (mid-Holocene minus pre-industrial). (a) Difference in the average austral summer (December to February [DJF]) precipitation. Solid and dashed diagonal lines show the transect used in Figure 4 over the land and ocean component of the South Atlantic Convergence Zone (SACZ) respectively. Dotted gray line indicates the climatological position of the SACZ in the modern-day simulation. (b) Background colors indicate the change in DJF sea-level pressure. Vectors represent the change in average DJF winds. (c) Background colors indicates the change in the mean $\delta^{18}O$ simulated by the ECHAM4.6 (based on monthly precipitation-weighted $\delta^{18}O$). The colored symbols indicate $\delta^{18}O$ difference between the mid-Holocene and pre-industrial in speleothem (triangle) and ice-core (square) records listed in Table S3 in Supporting Information S1. Values next to each symbol is the observed difference in the $\delta^{18}O$ value between the mid-Holocene and pre-industrial. Dotted regions in panels (a, b) indicate where the difference is significant at a 95% confidence level. (d) Contours show the stream function (10^{-7} m^2s^{-1}) calculated by the U and V winds in the mid-Holocene scenario (red) and pre-industrial scenario (black). The stream function is used to highlight changes in the subtropical high intensity and position between the two scenarios.

the mid-Holocene timeframe (Figure 2) (Text S1 and Table S2 in Supporting Information S1). The simulated $\delta^{18}O$ values are additionally compared to the observed $\delta^{18}O$ difference in regional proxy records (Text S1 and Table S3 in Supporting Information S1). To further investigate the SACZ dipole response, the precipitation change across the SACZ is highlighted by comparing the precipitation change along two southwest to northeast transects that are perpendicular to the SACZ indicated by the black solid and dashed lines in Figure 3a: one along the eastern edge of the continent (between 10°S, 38°W and 30°S, 58°W) and the other the ocean (between 18°S, 22°W and 38°S, 42°W), following the approach used by Zilli et al. (2019).

3. Results

Compared to modern-day reanalysis data, the ECHAM4.6–slab ocean model is able to adequately simulate the large-scale precipitation features that characterize the SASM season, including the deep convection over the Amazon and the SACZ as a diagonal rainfall band extending southeast from the western Amazon into the tropical Atlantic off the coast of southern Brazil (Figure S1 in Supporting Information S1). The mid-Holocene scenario

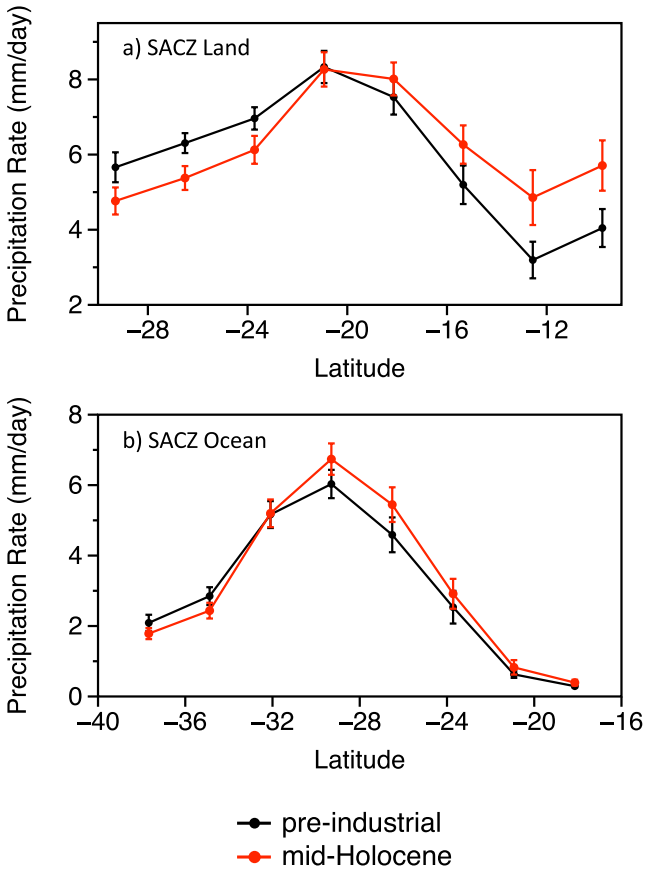

Figure 4. Average austral summer precipitation rates across the South Atlantic Convergence Zone (SACZ) in the mid-Holocene (red) and pre-industrial simulations (black). (a) Precipitation along a transect perpendicular to the SACZ over land (~10°S, 38°W to ~30°S, 58°W). Error bars indicates the 95% confidence level based on the Student's t-distribution. (b) Same as (a) but for the oceanic component of the SACZ (~18°S, 22°W to ~38°S, 42°W). Locations for the transects are plotted in Figure 3a.

generates higher austral summer precipitation along the northeastern coast of Brazil and western tropical Atlantic than in the modern-day simulation (Figure 3a). In addition to the previously noted southward intensification of the ITCZ over the Atlantic (e.g., Chiessi et al., 2021) and the weakened Nordeste Low (e.g., Cruz et al., 2009) (Figure S2 in Supporting Information S1), the higher precipitation off the northeastern coast is associated with an intensified convection over the northern margin of the SACZ. This northward intensification is further evident in the 850 hPa wind field (Figure 3b) that shows a prominent cyclonic anomaly and lower sea-level pressures (SLP) over the ocean adjacent to southeastern Brazil during the mid-Holocene (centered around 25°S, 35°W in Figure 3b), related to the ascending motion caused by increased convective activity in the SACZ.

Lower DJF precipitation in the mid-Holocene scenario is simulated along the western Amazon and Andes to SESA. The reduction in precipitation over SESA is related to an overall weaker summer monsoon and the resulting reduction in the amount of moisture delivered by the weakened LLJ. Furthermore, a higher SLP over northern Argentina (due to a weaker CL system) and the reduced SLP around the SACZ region creates a pressure gradient that favors a more eastward deflection of the LLJ toward the SACZ whilst diminishing the intensity of the LLJ's southward penetration to the subtropics (seen in the wind field change in Figure 3b).

The north–south anti-phased anomalies in Figure 3a are bisected by a diagonal zone with little-to-no precipitation change that runs approximately along the central axis of the SACZ. This implies that despite precipitation changes to the north and south of the SACZ, precipitation near the central axis remained relatively constant. Overall, the simulated change in mid-Holocene precipitation shows a broad agreement with hydroclimate proxy interpretations, particularly in the northeastern coast (e.g., Chiessi et al., 2021; Cruz et al., 2009) and SESA (e.g., Behling et al., 2001; X. Wang et al., 2007; Ward et al., 2019) (Figures 2 and 3a).

The northeast–southwest anti-phased pattern is mirrored in the annual mean $\delta^{18}O$ based on monthly precipitation-weighted $\delta^{18}O$ (Figure 3c). The changes in the annual mean $\delta^{18}O$ is dominantly caused by changes related to austral summertime precipitation (Figure S3 in Supporting Information S1). The precipitation $\delta^{18}O$ changes in the mid-Holocene compared to the pre-industrial climate are negative over the northeastern coast and positive over the western Amazon to SESA. The general correspondence between the simulated changes in precipitation amount and $\delta^{18}O$ values is consistent with the "amount effect" mechanism that is commonly used to interpret $\delta^{18}O$ records in the tropics. Although simulated $\delta^{18}O$ shows a similar spatial pattern in terms of the direction of $\delta^{18}O$ change exhibited by the proxy records, the magnitude of $\delta^{18}O$ change is underestimated in the model. For instance, the Rio Grande do Norte speleothem record along the northeastern coast (Figure 3c) (Cruz et al., 2009) shows a $\delta^{18}O$ difference of $-4.2‰$ compared to the $>-1‰$ change in the model. Similarly, in the Botuvera Cave speleothem record in southern Brazil, the difference is up to 2.9‰, compared to <0.3‰ change in the model. This issue is not unique to the ECHAM4.6, as it has been noted by other isotope-enabled simulations (e.g., Cauquoin et al., 2019; Tabor et al., 2020) and is likely due to a climate model's tendency to underestimate summer rainfall amount across the Amazon. Nevertheless, although the absolute values of $\delta^{18}O$ may not be directly comparable to the $\delta^{18}O$ proxy records, the direction of precipitation change is captured in the model.

4. SACZ Mid-Holocene Response

4.1. Description of SACZ Response

The austral summer precipitation across the SACZ axis shows that the latitudinal position of the peak SACZ rainfall does not change in the mid-Holocene compared to the modern (Figure 4), suggesting that there is no

latitudinal displacement of the core SACZ axis, or at least that no latitudinal movement can be detected at the model resolution. However, there is a clear latitudinal difference in precipitation response over the land component of the SACZ during the austral summer: toward the equator, rainfall rates were higher during the mid-Holocene than the pre-industrial, while the opposite is true along the southern margin. In effect, continental precipitation in the mid-Holocene is distributed more symmetrically around the axis of maximum precipitation than it is in the modern-day simulation (Figure 4a). A similar transect across the oceanic component of the SACZ shows that the latitudinal position of peak precipitation remains the same as well, suggesting that, similar to the land component, there is no shift in the core SACZ position (Figure 4b). However, the magnitude of rainfall change along the flanks of the SACZ is less than that seen on the land transect, which is due to the reduced contribution from the LLJ and ITCZ moisture. The stationary latitudinal position of the peak rainfall over both land and ocean between the mid-Holocene and the present, therefore, suggests that the SACZ responded in a north–south dipole rather than an overall latitudinal displacement of the core SACZ axis.

4.2. Mechanisms for the Dipole SACZ Response

The distribution of the precipitation in the SACZ is closely associated with the two moisture sources that converge to form the SACZ, that is, the westerly inflow from continental moisture flux and the northeasterly flow from the western flank of the SASH (Kodama, 1993; Nogués-Paegle & Mo, 1997; Saulo et al., 2000). The westerly continental flux is affected by the direction and intensity of the LLJ (Boers et al., 2014; Zilli et al., 2019). Modern-day observations have shown that when the LLJ has a strong eastward component, moisture is channeled toward the SACZ over central Brazil. The intensified convergence over central Brazil results in a compensatory subsidence over the southwest that suppresses rainfall in SESA (Gandu & Silva Dias, 1998), as well as limiting the southward extent of the LLJ (Robertson & Mechoso, 2000). In the opposite phase, the LLJ has a stronger southward component, bringing moisture toward Argentina and SESA, with subsidence located over eastern Brazil. Therefore, the intensified convection over SESA is associated with a weaker SACZ over central Brazil. In our mid-Holocene simulations, a higher pressure over northern Argentina and SESA associated with the weakened CL (due to less intensive Amazonian convection) and the low pressure region under the SACZ (Figure 3b) inhibits the southwards flow and instead forces Amazonian moisture eastwards toward the SACZ over central-eastern Brazil, rather than allowing the LLJ to prevail southwards over SESA. During the pre-industrial, the opposite is true: a deeper CL resulting from enhanced SASM convection promotes a stronger LLJ over the SESA and a weaker SACZ over central Brazil.

Precipitation intensity along the northern margin of the SACZ is largely dependent on the SASH circulation (Zilli et al., 2019). During austral summer, the SASH is sustained by the Southern Hemisphere monsoons and the zonal SST gradient across the Atlantic (Miyasaka & Nakamura, 2010; Reboita et al., 2019; Seager et al., 2003). The SASM is also important in sustaining the SASH as the Kelvin wave response to monsoon convection toward the east contributes to the subsidence that enhances the subtropical anticyclone (Gill, 1980; Rodwell & Hoskins, 2001; Seager et al., 2003). In the mid-Holocene scenario, there is a contraction of the SASH along its western boundary (Figure 3d), which is consistent with a reduced SASM intensity and subsidence over the Atlantic. The western contraction of the SASH steepens the zonal pressure gradient across the Atlantic, causing an acceleration of wind speeds along the northern and western flanks of the SASH (Figure 3b) (Pontes et al., 2020; Zilli et al., 2019). This northerly flow gives rise to the prominent low-level convergence along the northeastern coast and along the equatorward margin of the SACZ. The stronger easterly flow across the tropical Atlantic leading to SACZ convergence is similar to the previous investigations by Liu and Battisti (2015), although the authors attributed the flow instead to a Rossby wave response to South African precipitation. The strengthening due to increased convective activity in the SACZ, contributes to the prominent cyclonic anomaly over the ocean adjacent to southeastern Brazil during the mid-Holocene (i.e., the cyclonic anomaly centered around 25°S, 35°W in Figure 3b). Cyclogenesis over this region has previously been noted by Grimm et al. (2007) and Nielsen et al. (2019) to correspond with northernmost SACZ conditions.

5. Conclusion

The simulations and hydroclimate records both show that, in response to changes in insolation from the mid-Holocene to today, the centroid of SACZ precipitation shifts northward, resulting in a north–south pattern in precipitation anomalies, rather than an overall latitudinal migration of the SACZ. One key goal of this study

is to understand how the SACZ was strengthened during the mid-Holocene. Our simulations suggest that the northward intensification of the SACZ during the mid-Holocene was due to a stronger easterly circulation across the tropical Atlantic producing intense moisture convergence in the equatorward margin of the SACZ. The southwards transport of continental moisture along the LLJ is concurrently reduced due to a weakened CL, and is instead channeled eastwards toward the SACZ which limits the penetration of moisture toward SESA. This study therefore provides new insight to the behaviors of the SACZ during the mid-Holocene and aids the further interpretation of $\delta^{18}O$ proxy records in the region.

Data Availability Statement

The results of the ECHAM4.6 model simulation in this study is available at Wong (2023a, 2023b), for the pre-industrial and mid-Holocene scenarios, respectively. The ERA5 data set is available in Hersbach et al. (2023). The data set containing paleoclimate records used in Figure 2 is compiled in Gorenstein et al. (2022). The Angelica Cave speleothem $\delta^{18}O$ record is available at Wong et al. (2021a).

Acknowledgments
This research was supported by the Earth Observatory of Singapore via its funding from the National Research Foundation Singapore (NRF), the Singapore Ministry of Education (MOE) under the Research Centres of Excellence initiative and an MOE Tier 2 Grant (MOE2019-T2-1-174 (S) to X.W.). M.W. is supported by a Nanyang Graduate President's Scholarship and a Stephen Riady Geoscience Scholarship. This work comprises EOS contribution number 554.

References

Battisti, D. S., Ding, Q., & Roe, G. H. (2014). Coherent pan-Asian climatic and isotopic response to orbital forcing of tropical insolation. *Journal of Geophysical Research: Atmospheres*, *119*(21), 11997–12020. https://doi.org/10.1002/2014JD021960

Behling, H., Bauermann, S. G., & Pereira Neves, P. C. (2001). Holocene environmental changes in the São Francisco de Paula region, southern Brazil. *Journal of South American Earth Sciences*, *14*(6), 631–639. https://doi.org/10.1016/S0895-9811(01)00040-2

Bernal, J. P., Cruz, F. W., Stríkis, N. M., Wang, X., Deininger, M., Catunda, M. C. A., et al. (2016). High-resolution Holocene South American monsoon history recorded by a speleothem from Botuverá Cave, Brazil. *Earth and Planetary Science Letters*, *450*, 186–196. https://doi.org/10.1016/j.epsl.2016.06.008

Boers, N., Rheinwalt, A., Bookhagen, B., Barbosa, H. M. J., Marwan, N., Marengo, J., & Kurths, J. (2014). The South American rainfall dipole: A complex network analysis of extreme events. *Geophysical Research Letters*, *41*(20), 7397–7405. https://doi.org/10.1002/2014GL061829

Carvalho, L. M. V., Jones, C., & Liebmann, B. (2004). The South Atlantic convergence zone: Intensity, form, persistence, and relationships with intraseasonal to interannual activity and extreme rainfall. *Journal of Climate*, *17*(1), 88–108. https://doi.org/10.1175/1520-0442(2004)017<0088:Tsaczi>2.0.Co;2

Cauquoin, A., Werner, M., & Lohmann, G. (2019). Water isotopes – Climate relationships for the mid-Holocene and preindustrial period simulated with an isotope-enabled version of MPI-ESM. *Climate of the Past*, *15*(6), 1913–1937. https://doi.org/10.5194/cp-15-1913-2019

Chiessi, C. M., Mulitza, S., Taniguchi, N. K., Prange, M., Campos, M. C., Häggi, C., et al. (2021). Mid- to late Holocene contraction of the intertropical convergence zone over northeastern South America. *Paleoceanography and Paleoclimatology*, *36*(4), e2020PA003936. https://doi.org/10.1029/2020PA003936

Cook, K. H., Hsieh, J.-S., & Hagos, S. M. (2004). The Africa–South America intercontinental teleconnection. *Journal of Climate*, *17*(14), 2851–2865. https://doi.org/10.1175/1520-0442(2004)017<2851:Taait>2.0.Co;2

Cruz, F. W., Vuille, M., Burns, S. J., Wang, X., Cheng, H., Werner, M., et al. (2009). Orbitally driven east–west antiphasing of South American precipitation. *Nature Geoscience*, *2*(3), 210–214. https://doi.org/10.1038/ngeo444

De Souza, E. B., & Ambrizzi, T. (2006). Modulation of the intraseasonal rainfall over tropical Brazil by the Madden–Julian oscillation. *International Journal of Climatology*, *26*(13), 1759–1776. https://doi.org/10.1002/joc.1331

Gandu, A. W., & Silva Dias, P. L. (1998). Impact of tropical heat sources on the South American tropospheric upper circulation and subsidence. *Journal of Geophysical Research*, *103*(D6), 6001–6015. https://doi.org/10.1029/97JD03114

Gill, A. E. (1980). Some simple solutions for heat-induced tropical circulation (pp. 447–462).

Gorenstein, I., Prado, L. F., Bianchini, P. R., Wainer, I., Griffiths, M. L., Pausata, F. S. R., & Yokoyama, E. (2022). A fully calibrated and updated mid-Holocene climate reconstruction for Eastern South America [Dataset]. Quaternary Science Reviews, *292*, 107646. https://doi.org/10.1016/j.quascirev.2022.107646

Grimm, A., Pal, J., & Giorgi, F. (2007). Connection between spring conditions and peak summer monsoon rainfall in South America: Role of soil moisture, surface temperature, and topography in eastern Brazil. *Journal of Climate*, *20*(24), 5929–5945. https://doi.org/10.1175/2007JCLI1684.1

Hersbach, H., Bell, B., Berrisford, P., Biavati, G., Horányi, A., Muñoz Sabater, J., et al. (2023). ERA5 monthly averaged data on single levels from 1940 to present [Dataset]. Copernicus Climate Change Service (C3S) Climate Data Store (CDS). https://doi.org/10.24381/cds.f17050d7

Hoffmann, G., Werner, M., & Heimann, M. (1998). Water isotope module of the ECHAM atmospheric general circulation model: A study on timescales from days to several years. *Journal of Geophysical Research*, *103*(D14), 16871–16896. https://doi.org/10.1029/98JD00423

Jorgetti, T., da Silva Dias, P. L., & de Freitas, E. D. (2013). The relationship between South Atlantic SST and SACZ intensity and positioning. *Climate Dynamics*, *42*(11–12), 3077–3086. https://doi.org/10.1007/s00382-013-1998-z

Kodama, Y.-M. (1993). Large-scale common features of sub-tropical convergence zones (the Baiu Frontal zone, the SPCZ, and the SACZ) Part II: Conditions of the circulations for generating the STCZs. *Journal of the Meteorological Society of Japan*, *71*(5), 581–610. https://doi.org/10.2151/JMSJ1965.71.5_581

Laskar, J., Robutel, P., Joutel, F., Gastineau, M., Correia, A., & Levrard, B. (2004). A long-term numerical solution for the insolation quantities of the Earth. *Astronomy & Astrophysics*, *428*(1), 261–285. https://doi.org/10.1051/0004-6361:20041335

Liebmann, B., Kiladis, G. N., Vera, C. S., Saulo, A. C., & Carvalho, L. M. V. (2004). Subseasonal variations of rainfall in South America in the vicinity of the low-level jet east of the Andes and comparison to those in the South Atlantic convergence zone. *Journal of Climate*, *17*(19), 3829–3842. https://doi.org/10.1175/1520-0442(2004)017<3829:Svoris>2.0.Co;2

Liu, X., & Battisti, D. S. (2015). The influence of orbital forcing of tropical insolation on the climate and isotopic composition of precipitation in South America. *Journal of Climate*, *28*(12), 4841–4862. https://doi.org/10.1175/jcli-d-14-00639.1

Miyasaka, T., & Nakamura, H. (2010). Structure and mechanisms of the Southern Hemisphere summertime subtropical anticyclones. *Journal of Climate*, *23*(8), 2115–2130. https://doi.org/10.1175/2009jcli3008.1

Nielsen, D. M., Belém, A. L., Marton, E., & Cataldi, M. (2019). Dynamics-based regression models for the South Atlantic convergence zone. *Climate Dynamics*, *52*(9–10), 5527–5553. https://doi.org/10.1007/s00382-018-4460-4

Nogués-Paegle, J., & Mo, K. C. (1997). Alternating wet and dry conditions over South America during summer. *Monthly Weather Review*, *125*(2), 279–291. https://doi.org/10.1175/1520-0493(1997)125<0279:Awadco>2.0.Co;2

Otto-Bliesner, B. L., Braconnot, P., Harrison, S. P., Lunt, D. J., Abe-Ouchi, A., Albani, S., et al. (2017). The PMIP4 contribution to CMIP6 – Part 2: Two interglacials, scientific objective and experimental design for Holocene and Last Interglacial simulations. *Geoscientific Model Development*, *10*(11), 3979–4003. https://doi.org/10.5194/gmd-10-3979-2017

Perez Filho, A., Moreira, V., Lämmle, L., Souza, A., Torres, B., Aderaldo, P., et al. (2022). Genesis and distribution of low fluvial terraces formed by Holocene climate pulses in Brazil. *Water*, *14*(19), 2977. https://doi.org/10.3390/w14192977

Pontes, G., Wainer, I., Taschetto, A., Gupta, A., Abe-Ouchi, A., Brady, E., et al. (2020). Drier tropical and subtropical southern Hemisphere in the mid-Pliocene warm period. *Scientific Reports*, *10*(1), 13458. https://doi.org/10.1038/s41598-020-68884-5

Prado, L., Wainer, I., Chiessi, C., Ledru, M.-P., & Turcq, B. (2013). A mid-Holocene climate reconstruction for Eastern South America. *Climate of the Past*, *9*(5), 2117–2133. https://doi.org/10.5194/cp-9-2117-2013

Reboita, M. S., Ambrizzi, T., Silva, B. A., Pinheiro, R. F., & da Rocha, R. P. (2019). The South Atlantic subtropical anticyclone: Present and future climate. *Frontiers in Earth Science*, *7*, 8. https://doi.org/10.3389/feart.2019.00008

Robertson, A. W., & Mechoso, C. R. (2000). Interannual and interdecadal variability of the South Atlantic convergence zone. *Monthly Weather Review*, *128*(8), 2947–2957. https://doi.org/10.1175/1520-0493(2000)128<2947:Iaivot>2.0.Co;2

Rodwell, M. J., & Hoskins, B. J. (2001). Subtropical anticyclones and summer monsoons. *Journal of Climate*, *14*(15), 3192–3211. https://doi.org/10.1175/1520-0442(2001)014<3192:Saasm>2.0.Co;2

Roeckner, E., Arpe, K., Bengtsson, L., Christoph, M., Claussen, M., Dümenil, L., et al. (1996). The atmospheric general circulation model ECHAM-4: Model description and simulation of present-day climate. https://doi.org/10.17617/2.1781494

Samanta, D., Karnauskas, K. B., & Goodkin, N. F. (2019). Tropical Pacific SST and ITCZ biases in climate models: Double trouble for future rainfall projections? *Geophysical Research Letters*, *46*(4), 2242–2252. https://doi.org/10.1029/2018GL081363

Saulo, A. C., Nicolini, M., & Chou, S. C. (2000). Model characterization of the South American low-level flow during the 1997–1998 spring–summer season. *Climate Dynamics*, *16*(10–11), 867–881. https://doi.org/10.1007/s003820000085

Seager, R., Murtugudde, R., Naik, N., Clement, A., Gordon, N., & Miller, J. (2003). Air–sea interaction and the seasonal cycle of the subtropical anticyclones. *Journal of Climate*, *16*(12), 1948–1966. https://doi.org/10.1175/1520-0442(2003)016<1948:Aiatsc>2.0.Co;2

Smith, R. J., & Mayle, F. E. (2018). Impact of mid- to late Holocene precipitation changes on vegetation across lowland tropical South America: A paleo-data synthesis. *Quaternary Research*, *89*(1), 134–155. https://doi.org/10.1017/qua.2017.89

Strikis, N. M., Cruz, F. W., Cheng, H., Karmann, I., Edwards, R. L., Vuille, M., et al. (2011). Abrupt variations in South American monsoon rainfall during the Holocene based on a speleothem record from central-eastern Brazil. *Geology*, *39*(11), 1075–1078. https://doi.org/10.1130/g32098.1

Tabor, C., Otto-Bliesner, B., & Liu, Z. (2020). Speleothems of South American and Asian monsoons influenced by a green Sahara. *Geophysical Research Letters*, *47*(22), e2020GL089695. https://doi.org/10.1029/2020GL089695

Wang, C., Zhang, L., Lee, S.-K., Wu, L., & Mechoso, C. R. (2014). A global perspective on CMIP5 climate model biases. *Nature Climate Change*, *4*(3), 201–205. https://doi.org/10.1038/nclimate2118

Wang, X., Auler, A. S., Edwards, R. L., Cheng, H., Ito, E., & Solheid, M. (2006). Interhemispheric anti-phasing of rainfall during the last glacial period. *Quaternary Science Reviews*, *25*(23–24), 3391–3403. https://doi.org/10.1016/j.quascirev.2006.02.009

Wang, X., Auler, A. S., Edwards, R. L., Cheng, H., Ito, E., Wang, Y., et al. (2007). Millennial-scale precipitation changes in southern Brazil over the past 90,000 years. *Geophysical Research Letters*, *34*(23), L23701. https://doi.org/10.1029/2007GL031149

Ward, B. M., Wong, C. I., Novello, V. F., McGee, D., Santos, R. V., Silva, L. C. R., et al. (2019). Reconstruction of Holocene coupling between the South American Monsoon System and local moisture variability from speleothem $\delta^{18}O$ and $^{87}Sr/^{86}Sr$ records. *Quaternary Science Reviews*, *210*, 51–63. https://doi.org/10.1016/j.quascirev.2019.02.019

Wong, M. (2023a). ECHAM4.6-slab ocean model mid-Holocene simulation output [Dataset]. V1 ed. DR-NTU. https://doi.org/10.21979/N9/KA0RRM

Wong, M. (2023b). ECHAM4.6-slab ocean model pre-industrial simulation output [Dataset]. V1 ed. DR-NTU. https://doi.org/10.21979/N9/YGZHVQ

Wong, M., Wang, X., Latrubesse, E. M., He, S., & Bayer, M. (2021a). Stable isotope ($\delta^{18}O$, $\delta^{13}C$) results of speleothems from Angelica Cave (central Brazil) [Dataset]. Pangaea. https://doi.org/10.1594/PANGAEA.938676

Wong, M., Wang, X., Latrubesse, E. M., He, S., & Bayer, M. (2021b). Variations in the South Atlantic convergence zone over the mid-to-late Holocene inferred from speleothem $\delta^{18}O$ in central Brazil. *Quaternary Science Reviews*, *270*, 107178. https://doi.org/10.1016/j.quascirev.2021.107178

Zilli, M. T., Carvalho, L. M. V., & Lintner, B. R. (2019). The poleward shift of South Atlantic Convergence Zone in recent decades. *Climate Dynamics*, *52*(5–6), 2545–2563. https://doi.org/10.1007/s00382-018-4277-1

References From the Supporting Information

Absy, M. L., Cleef, A., Fournier, M., Martin, L., Servant, M., Sifeddine, A., et al. (1991). Mise en évidence de quatre phases d'ouverture de la forêt dense dans le Sud-Est de l'Amazonie au cours des 60 000 dernières années: Première comparaison avec d'autres régions tropicales. *Comptes Rendus de l'Académie des Sciences.Série 2 : Mécanique.*, *312*, 673–678.

Arz, H. W., Gerhardt, S., Pätzold, J., & Röhl, U. (2001). Millennial-scale changes of surface- and deep-water flow in the western tropical Atlantic linked to Northern Hemisphere high-latitude climate during the Holocene. *Geology*, *29*(3), 239–242. https://doi.org/10.1130/0091-7613(2001)029<0239:Mscosa>2.0.Co;2

Arz, H. W., Pätzold, J., & Wefer, G. (1998). Correlated millennial-scale changes in surface hydrography and terrigenous sediment yield inferred from last-glacial marine deposits off northeastern Brazil. *Quaternary Research*, *50*(2), 157–166. https://doi.org/10.1006/qres.1998.1992

Barberi, M., Salgado-Labouriau, M., & Suguio, K. (2000). Paleovegetation and paleoclimate of "vereda de Águas Emendadas". *central Brazil. Journal of South American Earth Sciences - J S AMER EARTH SCI*, *13*(3), 241–254. https://doi.org/10.1016/S0895-9811(00)00022-5

Barreto, E. A. D. S., & Cruz, F. W. (2010). Reconstituição da pluviosidade da Chapada Diamantina (BA) durante o Quaternário tardio através de registros isotópicos (O e C) em estalagmites.

Behling, H. (1995). A high resolution Holocene pollen record from Lago do Pires, SE Brazil: Vegetation, climate and fire history. *Journal of Paleolimnology*, *14*(3), 253–268. https://doi.org/10.1007/BF00682427

Behling, H. (1997). Late Quaternary vegetation, climate and fire history of the Araucaria forest and Campos region from Serra Campos Gerais, Paraná State (South Brazil). *Review of Palaeobotany and Palynology*, *97*(1–2), 109–121. https://doi.org/10.1016/s0034-6667(96)00065-6
Behling, H. (2001). Late Quaternary environmental changes in the Lagoa da Curuça region (eastern Amazonia, Brazil) and evidence of Podocarpus in the Amazon lowland. *Vegetation History and Archaeobotany*, *10*(3), 175–183. https://doi.org/10.1007/PL00006929
Behling, H. (2003). Late glacial and Holocene vegetation, climate and fire history inferred from Lagoa Nova in the southeastern Brazilian lowland. *Vegetation History and Archaeobotany*, *12*(4), 263–270. https://doi.org/10.1007/s00334-003-0020-9
Behling, H. (2007). Late Quaternary vegetation, fire and climate dynamics of Serra do Araçatuba in the Atlantic coastal mountains of Paraná State, southern Brazil. *Vegetation History and Archaeobotany*, *16*(2–3), 77–85. https://doi.org/10.1007/s00334-006-0078-2
Behling, H., Carlos Berrio, J., & Hooghiemstra, H. (1999). Late Quaternary pollen records from the middle Caquetá river basin in central Colombian Amazon. *Palaeogeography, Palaeoclimatology, Palaeoecology*, *145*(1–3), 193–213. https://doi.org/10.1016/S0031-0182(98)00105-9
Behling, H., & Costa, M. L. (1997). Studies on Holocene tropical vegetation mangrove and coast environments in the state of Maranhão, NE Brazil. *Quaternary of South America and Antarctic Peninsula*, *10*, 93–118.
Behling, H., & da Costa, M. L. (2000). Holocene environmental changes from the Rio Curuá record in the Caxiuanã region, eastern Amazon basin. *Quaternary Research*, *53*(3), 369–377. https://doi.org/10.1006/qres.1999.2117
Behling, H., Dupont, L., DeForest Safford, H., & Wefer, G. (2007). Late Quaternary vegetation and climate dynamics in the Serra da Bocaina, southeastern Brazil. *Quaternary International*, *161*(1), 22–31. https://doi.org/10.1016/j.quaint.2006.10.021
Behling, H., & Lima da Costa, M. (2001). Holocene vegetational and coastal environmental changes from the Lago Crispim record in northeastern Pará State, eastern Amazonia. *Review of Palaeobotany and Palynology*, *114*(3–4), 145–155. https://doi.org/10.1016/s0034-6667(01)00044-6
Behling, H., & Negrelle, R. R. B. (2001). Tropical rain forest and climate dynamics of the Atlantic lowland, southern Brazil, during the late quaternary. *Quaternary Research*, *56*(3), 383–389. https://doi.org/10.1006/qres.2001.2264
Behling, H., Pillar, V. D., & Bauermann, S. G. (2005). Late Quaternary grassland (Campos), gallery forest, fire and climate dynamics, studied by pollen, charcoal and multivariate analysis of the São Francisco de Assis core in western Rio Grande do Sul (southern Brazil). *Review of Palaeobotany and Palynology*, *133*(3–4), 235–248. https://doi.org/10.1016/j.revpalbo.2004.10.004
Behling, H., Pillar, V. D. P., Orlóci, L., & Bauermann, S. G. (2004). Late Quaternary Araucaria forest, grassland (Campos), fire and climate dynamics, studied by high-resolution pollen, charcoal and multivariate analysis of the Cambará do Sul core in southern Brazil. *Palaeogeography, Palaeoclimatology, Palaeoecology*, *203*(3–4), 277–297. https://doi.org/10.1016/s0031-0182(03)00687-4
Behling, H., & Safford, H. (2009). Late-glacial and Holocene vegetation, climate and fire dynamics in the Serra dos Orgaos, Rio de Janeiro State, southeastern Brazil. *Global Change Biology*, *16*(6), 1661–1671. https://doi.org/10.1111/j.1365-2486.2009.02029.x
Breukelen, M. R., Vonhof, H., Hellstrom, J., Wester, W. C. G., & Kroon, D. (2008). Fossil dripwater in stalagmites reveals Holocene temperature and rainfall variation in Amazonia. *Earth and Planetary Science Letters*, *275*(1–2), 54–60. https://doi.org/10.1016/j.epsl.2008.07.060
Brugger, S. O., Gobet, E., van Leeuwen, J. F. N., Ledru, M.-P., Colombaroli, D., van der Knaap, W. O., et al. (2016). Long-term man–environment interactions in the Bolivian Amazon: 8000 years of vegetation dynamics. *Quaternary Science Reviews*, *132*, 114–128. https://doi.org/10.1016/j.quascirev.2015.11.001
Bush, M. B., Miller, M. C., De Oliveira, P. E., & Colinvaux, P. A. (2000). Two histories of environmental change and human disturbance in eastern lowland Amazonia. *The Holocene*, *10*(5), 543–553. https://doi.org/10.1191/095968300672647521
Bush, M. B., Silman, M. R., de Toledo, M. B., Listopad, C., Gosling, W. D., Williams, C., et al. (2007). Holocene fire and occupation in Amazonia: Records from two lake districts. *Philosophical Transactions of the Royal Society B: Biological Sciences*, *362*(1478), 209–218. https://doi.org/10.1098/rstb.2006.1980
Bustamante, M. G., Cruz, F. W., Vuille, M., Apaéstegui, J., Strikis, N., Panizo, G., et al. (2016). Holocene changes in monsoon precipitation in the Andes of NE Peru based on $\delta^{18}O$ speleothem records. *Quaternary Science Reviews*, *146*, 274–287. https://doi.org/10.1016/j.quascirev.2016.05.023
Calegari, M. R., Madella, M., Vidal-Torrado, P., Pessenda, L. C. R., & Marques, F. A. (2013). Combining phytoliths and $\delta^{13}C$ matter in Holocene palaeoenvironmental studies of tropical soils: An example of an Oxisol in Brazil. *Quaternary International*, *287*, 47–55. https://doi.org/10.1016/j.quaint.2011.11.012
Carson, J., Mayle, F., Whitney, B., Iriarte, J., & Soto, D. (2016). Pre-columbian ring ditch construction and land use on a 'chocolate forest island' in the Bolivian Amazon: PRE-COLUMBIAN 'chocolate forest islands' in BOLIVIAN amazon. *Journal of Quaternary Science*, *31*(4), 337–347. https://doi.org/10.1002/jqs.2835
Carson, J. F., Watling, J., Mayle, F. E., Whitney, B. S., Iriarte, J., Prümers, H., & Soto, J. D. (2015). Pre-Columbian land use in the ring-ditch region of the Bolivian Amazon. *The Holocene*, *25*(8), 1285–1300. https://doi.org/10.1177/0959683615581204
Carson, J. F., Whitney, B. S., Mayle, F. E., Iriarte, J., Prümers, H., Soto, J. D., & Watling, J. (2014). Environmental impact of geometric earthwork construction in pre-Columbian Amazonia. *Proceedings of the National Academy of Sciences of the United States of America*, *111*(29), 10497–10502. https://doi.org/10.1073/pnas.1321770111
Cassino, R. F., Ledru, M.-P., Santos, R. D. A., & Favier, C. (2020). Vegetation and fire variability in the central Cerrados (Brazil) during the Pleistocene-Holocene transition was influenced by oscillations in the SASM boundary belt. *Quaternary Science Reviews*, *232*, 106209. https://doi.org/10.1016/j.quascirev.2020.106209
Cassino, R. F., Martinho, C. T., & da Silva Caminha, S. A. F. (2018). A Late Quaternary palynological record of a palm swamp in the Cerrado of central Brazil interpreted using modern analog data. *Palaeogeography, Palaeoclimatology, Palaeoecology*, *490*, 1–16. https://doi.org/10.1016/j.palaeo.2017.08.036
Chiessi, C., Mulitza, S., Pätzold, J., & Wefer, G. (2010). How different proxies record precipitation variability over southeastern South America. *IOP Conference Series: Earth and Environmental Science*, *9*, 012007. https://doi.org/10.1088/1755-1315/9/1/012007
Cohen, M. C. L., Rossetti, D. F., Pessenda, L. C. R., Friaes, Y. S., & Oliveira, P. E. (2014). Late pleistocene glacial forest of Humaitá—Western Amazonia. *Palaeogeography, Palaeoclimatology, Palaeoecology*, *415*, 37–47. https://doi.org/10.1016/j.palaeo.2013.12.025
Colinvaux, P. A., Oliveira, P., Moreno, J. E., Miller, M., & Bush, M. (1996). A long pollen record from lowland Amazonia: Forest and cooling in glacial times. *Science*, *274*(5284), 85–88. https://doi.org/10.1126/science.274.5284.85
Comas-Bru, L., Rehfeld, K., Roesch, C., Amirnezhad-Mozhdehi, S., Harrison, S. P., Atsawawaranunt, K., et al. (2020). SISALv2: A comprehensive speleothem isotope database with multiple age–depth models. *Earth System Science Data*, *12*(4), 2579–2606. https://doi.org/10.5194/essd-12-2579-2020
Cruz, F. W., Burns, S. J., Jercinovic, M., Karmann, I., Sharp, W. D., & Vuille, M. (2007). Evidence of rainfall variations in Southern Brazil from trace element ratios (Mg/Ca and Sr/Ca) in a Late Pleistocene stalagmite. *Geochimica et Cosmochimica Acta*, *71*(9), 2250–2263. https://doi.org/10.1016/j.gca.2007.02.005

Cruz, F. W., Burns, S. J., Karmann, I., Sharp, W. D., & Vuille, M. (2006a). Reconstruction of regional atmospheric circulation features during the late Pleistocene in subtropical Brazil from oxygen isotope composition of speleothems. *Earth and Planetary Science Letters*, *248*(1–2), 495–507. https://doi.org/10.1016/j.epsl.2006.06.019

Cruz, F. W., Burns, S. J., Karmann, I., Sharp, W. D., Vuille, M., Cardoso, A. O., et al. (2005). Insolation-driven changes in atmospheric circulation over the past 116,000 years in subtropical Brazil. *Nature*, *434*(7029), 63–66. https://doi.org/10.1038/nature03365

Cruz, F. W., Burns, S. J., Karmann, I., Sharp, W. D., Vuille, M., & Ferrari, J. A. (2006b). A stalagmite record of changes in atmospheric circulation and soil processes in the Brazilian subtropics during the Late Pleistocene. *Quaternary Science Reviews*, *25*(21–22), 2749–2761. https://doi.org/10.1016/j.quascirev.2006.02.019

de Freitas, H. A., Pessenda, L. C. R., Aravena, R., Gouveia, S. E. M., de Souza Ribeiro, A., & Boulet, R. (2001). Late quaternary vegetation dynamics in the southern Amazon basin inferred from carbon isotopes in soil organic matter. *Quaternary Research*, *55*(1), 39–46. https://doi.org/10.1006/qres.2000.2192

Deininger, M., Ward, B. M., Novello, V. F., & Cruz, F. W. (2019). Late quaternary variations in the South American monsoon system as inferred by speleothems—New perspectives using the SISAL database. *Quaternary*, *2*(1), 6. https://doi.org/10.3390/quat2010006

de Mahiques, M. M., Coaracy Wainer, I. K., Burone, L., Nagai, R., de Mello e Sousa, S. H., Lopes Figueira, R. C., et al. (2009). A high-resolution Holocene record on the Southern Brazilian shelf: Paleoenvironmental implications. *Quaternary International*, *206*(1–2), 52–61. https://doi.org/10.1016/j.quaint.2008.09.010

de Oliveira, M. A. T., Behling, H., & Pessenda, L. C. R. (2008a). Late-Pleistocene and mid-Holocene environmental changes in highland valley head areas of Santa Catarina state, Southern Brazil. *Journal of South American Earth Sciences*, *26*(1), 55–67. https://doi.org/10.1016/j.jsames.2008.03.001

de Oliveira, M. A. T., Behling, H., Pessenda, L. C. R., & de Lima, G. L. (2008b). Stratigraphy of near-valley head quaternary deposits and evidence of climate-driven slope-channel processes in southern Brazilian highlands. *Catena*, *75*(1), 77–92. https://doi.org/10.1016/j.catena.2008.04.003

De Oliveira, P. E. (1992). *A palynological record of late Quaternary vegetational and climatic change in southeastern Brazil, Book A palynological record of late Quaternary vegetational and climatic change in southeastern Brazil*. The Ohio State University.

De Oliveira, P. E., Barreto, A. M. F., & Suguio, K. (1999). Late Pleistocene/Holocene climatic and vegetational history of the Brazilian Caatinga: The fossil dunes of the middle São Francisco river. *Palaeogeography, Palaeoclimatology, Palaeoecology*, *152*(3–4), 319–337. https://doi.org/10.1016/S0031-0182(99)00061-9

De Toledo, M. B., & Bush, M. B. (2007). A mid-Holocene environmental change in Amazonian savannas. *Journal of Biogeography*, *34*(8), 1313–1326. https://doi.org/10.1111/j.1365-2699.2006.01606.x

Dümig, A., Schad, P., Rumpel, C., Dignac, M.-F., & Kögel-Knabner, I. (2008). Araucaria forest expansion on grassland in the southern Brazilian highlands as revealed by ^{14}C and $\delta^{13}C$ studies. *Geoderma*, *145*(1–2), 143–157. https://doi.org/10.1016/j.geoderma.2007.06.005

Enters, D., Behling, H., Mayr, C., Dupont, L., & Zolitschka, B. (2010). Holocene environmental dynamics of south-eastern Brazil recorded in laminated sediments of Lago Aleixo. *Journal of Paleolimnology*, *44*(1), 265–277. https://doi.org/10.1007/s10933-009-9402-z

Ferraz-vicentini, K. R., & Salgado-Labouriau, M. L. (1996). Palynological analysis of a palm swamp in Central Brazil. *Journal of South American Earth Sciences*, *9*(3–4), 207–219. https://doi.org/10.1016/0895-9811(96)00007-7

Fontes, D., Cordeiro, R. C., Martins, G. S., Behling, H., Turcq, B., Sifeddine, A., et al. (2017). Paleoenvironmental dynamics in South Amazonia, Brazil, during the last 35,000 years inferred from pollen and geochemical records of Lago do Saci. *Quaternary Science Reviews*, *173*, 161–180. https://doi.org/10.1016/j.quascirev.2017.08.021

Garcia, M., Oliveira, P., Siqueira, E., & Fernandes, R. (2004). A Holocene vegetational and climatic record from the Atlantic rainforest belt of coastal State of São Paulo, SE Brazil. *Review of Palaeobotany and Palynology*, *131*(3–4), 181–199. https://doi.org/10.1016/j.revpalbo.2004.03.007

Gouveia, S. E. M., Pessenda, L. C. R., Aravena, R., Boulet, R., Scheel-Ybert, R., Bendassoli, J. A., et al. (2002). Carbon isotopes in charcoal and soils in studies of paleovegetation and climate changes during the late Pleistocene and the Holocene in the southeast and centerwest regions of Brazil. *Global and Planetary Change*, *33*(1–2), 95–106. https://doi.org/10.1016/S0921-8181(02)00064-4

Groeneveld, J., & Chiessi, C. M. (2011). Mg/Ca of Globorotalia inflata as a recorder of permanent thermocline temperatures in the South Atlantic. *Paleoceanography*, *26*(2). https://doi.org/10.1029/2010PA001940

Guimarães, J. T. F., Sahoo, P. K., De Figueiredo, M. M. J. C., da Silva Lopes, K., Gastauer, M., Ramos, S. J., et al. (2021). Lake sedimentary processes and vegetation changes over the last 45k cal a bp in the uplands of south-eastern Amazonia. *Journal of Quaternary Science*, *36*(2), 255–272. https://doi.org/10.1002/jqs.3268

Hassan, G. S., Espinosa, M. A., & Isla, F. I. (2009). Diatom-based inference model for paleosalinity reconstructions in estuaries along the northeastern coast of Argentina. *Palaeogeography, Palaeoclimatology, Palaeoecology*, *275*(1–4), 77–91. https://doi.org/10.1016/j.palaeo.2009.02.020

Haug, G. H., Hughen, K. A., Sigman, D. M., Peterson, L. C., & Röhl, U. (2001). Southward migration of the intertropical convergence zone through the Holocene. *Science*, *293*(5533), 1304–1308. https://doi.org/10.1126/science.1059725

Hermanowski, B., Da Costa, M. L., & Behling, H. (2015). Possible linkages of palaeofires in southeast Amazonia to a changing climate since the Last Glacial Maximum. *Vegetation History and Archaeobotany*, *24*(2), 279–292. https://doi.org/10.1007/s00334-014-0472-0

Hoffmann, J., Bahr, A., Voigt, S., Schönfeld, J., Nürnberg, D., & Rethemeyer, J. (2014). Disentangling abrupt deglacial hydrological changes in northern South America: Insolation versus oceanic forcing. *Geology*, *42*(7), 579–582. https://doi.org/10.1130/g35562.1

Horák-Terra, I., Cortizas, A. M., Da Luz, C. F. P., Silva, A. C., Mighall, T., De Camargo, P. B., et al. (2020). Late quaternary vegetation and climate dynamics in central-eastern Brazil: Insights from a ∼35k cal a bp peat record in the Cerrado biome. *Journal of Quaternary Science*, *35*(5), 664–676. https://doi.org/10.1002/jqs.3209

Horák-Terra, I., Martínez Cortizas, A., da Luz, C. F. P., Rivas López, P., Silva, A. C., & Vidal-Torrado, P. (2015). Holocene climate change in central–eastern Brazil reconstructed using pollen and geochemical records of Pau de Fruta mire (Serra do Espinhaço Meridional, Minas Gerais). *Palaeogeography, Palaeoclimatology, Palaeoecology*, *437*, 117–131. https://doi.org/10.1016/j.palaeo.2015.07.027

Horbe, A., Behling, H., Nogueira, A., & Mapes, R. (2011). Environmental changes in the western Amazonia: Morphological framework, geochemistry, palynology and radiocarbon dating data. *Anais da Academia Brasileira de Ciências*, *83*(3), 863–874. https://doi.org/10.1590/S0001-37652011005000030

Iriarte, J. (2006). Vegetation and climate change since 14,810 14C yr B.P. in southeastern Uruguay and implications for the rise of early Formative societies. *Quaternary Research*, *65*(1), 20–32. https://doi.org/10.1016/j.yqres.2005.05.005

Iriarte, J., Holst, I., Marozzi, O., Listopad, C., Alonso, E., Rinderknecht, A., & Montaña, J. (2005). Evidence for cultivar adoption and emerging complexity during the mid-Holocene in the La Plata basin. *Nature*, *432*(7017), 614–617. https://doi.org/10.1038/nature02983

Irion, G., Bush, M. B., Nunes de Mello, J. A., Stüben, D., Neumann, T., Müller, G., et al. (2006). A multiproxy palaeoecological record of Holocene lake sediments from the Rio Tapajós, eastern Amazonia. *Palaeogeography, Palaeoclimatology, Palaeoecology*, *240*(3–4), 523–535. https://doi.org/10.1016/j.palaeo.2006.03.005

Jacob, J., Disnar, J. R., Boussafir, M., Sifeddine, A., Turcq, B., & Albuquerque, A. L. S. (2004). Major environmental changes recorded by lacustrine sedimentary organic matter since the last glacial maximum near the equator (Lagoa do Caco, NE Brazil). *Palaeogeography, Palaeoclimatology, Palaeoecology*, *205*(3–4), 183–197. https://doi.org/10.1016/j.palaeo.2003.12.005

Jaeschke, A., Rühlemann, C., Arz, H., Heil, G., & Lohmann, G. (2007). Coupling of millennial-scale changes in sea surface temperature and precipitation off northeastern Brazil with high-latitude climate shifts during the last glacial period. *Paleoceanography*, *22*(4), PA4206. https://doi.org/10.1029/2006pa001391

Jeske-Pieruschka, V., & Behling, H. (2012). Palaeoenvironmental history of the São Francisco de Paula region in southern Brazil during the late Quaternary inferred from the Rincão das Cabritas core. *The Holocene*, *22*(11), 1251–1262. https://doi.org/10.1177/0959683611414930

Jeske-Pieruschka, V., Pillar, V. D., De Oliveira, M. A. T., & Behling, H. (2013). New insights into vegetation, climate and fire history of southern Brazil revealed by a 40,000 year environmental record from the State Park Serra do Tabuleiro. *Vegetation History and Archaeobotany*, *22*(4), 299–314. https://doi.org/10.1007/s00334-012-0382-y

Kim, S.-T., & O'Neil, J. R. (1997). Equilibrium and nonequilibrium oxygen isotope effects in synthetic carbonates. *Geochimica et Cosmochimica Acta*, *61*(16), 3461–3475. https://doi.org/10.1016/S0016-7037(97)00169-5

Kim, S.-T., O'Neil, J. R., Hillaire-Marcel, C., & Mucci, A. (2007). Oxygen isotope fractionation between synthetic aragonite and water: Influence of temperature and Mg_2^+ concentration. *Geochimica et Cosmochimica Acta*, *71*(19), 4704–4715. https://doi.org/10.1016/j.gca.2007.04.019

Leal, M., & Lorscheitter, M. (2007). Plant succession in a forest on the lower northeast slope of Serra geral, Rio Grande do Sul, and holocene palaeoenvironments, southern Brazil. *Acta Botanica Brasilica*, *21*, 1–10. https://doi.org/10.1590/S0102-33062007000100001

Ledru, M.-P. (1993). Late quaternary environmental and climatic changes in Central Brazil. *Quaternary Research*, *39*(1), 90–98. https://doi.org/10.1006/qres.1993.1011

Ledru, M.-P., Ceccantini, G., Gouveia, S. E. M., López-Sáez, J. A., Pessenda, L. C. R., & Ribeiro, A. S. (2006). Millenial-scale climatic and vegetation changes in a northern Cerrado (northeast, Brazil) since the last glacial maximum. *Quaternary Science Reviews*, *25*(9–10), 1110–1126. https://doi.org/10.1016/j.quascirev.2005.10.005

Ledru, M.-P., Cordeiro, R. C., Dominguez, J. M. L., Martin, L., Mourguiart, P., Sifeddine, A., & Turcq, B. (2001). Late-glacial cooling in Amazonia inferred from pollen at Lagoa do Caçó, northern Brazil. *Quaternary Research*, *55*(1), 47–56. https://doi.org/10.1006/qres.2000.2187

Ledru, M.-P., Mourguiart, P., Ceccantini, G., Turcq, B., & Sifeddine, A. (2002). Tropical climates in the game of two hemispheres revealed by abrupt climatic change. *Geology*, *30*(3), 275–278. https://doi.org/10.1130/0091-7613(2002)030<0275:Tcitgo>2.0.Co;2

Ledru, M.-P., Mourguiart, P., & Riccomini, C. (2009). Related changes in biodiversity, insolation and climate in the Atlantic rainforest since the last interglacial. *Palaeogeography, Palaeoclimatology, Palaeoecology*, *271*(1–2), 140–152. https://doi.org/10.1016/j.palaeo.2008.10.008

Ledru, M.-P., Rousseau, D.-D., Cruz, F., Riccomini, C., Karmann, I., & Martin, L. (2005). Paleoclimate changes during the last 100,000 yr from a record in the Brazilian Atlantic rainforest region and interhemispheric comparison. *Quaternary Research*, *64*(3), 444–450. https://doi.org/10.1016/j.yqres.2005.08.006

Leonhardt, A., & Lorscheitter, M. L. (2010). The last 25,000 years in the eastern plateau of southern Brazil according to Alpes de São Francisco record. *Journal of South American Earth Sciences*, *29*(2), 454–463. https://doi.org/10.1016/j.jsames.2009.09.003

Lorente, F. L., Meyer, K. E. B., & Horn, A. H. (2010). Analise palinologica de vereda da fazenda urbano, municıpio de buritizeiro, minas gerais, brasil. *Geonomos*, *18*, 57–72. https://doi.org/10.18285/geonomos.v18i2.73

Maezumi, S. Y., Power, M. J., Mayle, F. E., McLauchlan, K. K., & Iriarte, J. (2015). Effects of past climate variability on fire and vegetation in the Cerrãdo savanna of the Huanchaca Mesetta, NE Bolivia. *Climate of the Past*, *11*(6), 835–853. https://doi.org/10.5194/cp-11-835-2015

Mayle, F. E., Burbridge, R., & Killeen, T. J. (2000). Millennial-scale dynamics of southern Amazonian rain forests. *Science*, *290*(5500), 2291–2294. https://doi.org/10.1126/science.290.5500.2291

Moreira, L. S., Moreira-Turcq, P., Turcq, B., Caquineau, S., & Cordeiro, R. C. (2012). Paleohydrological changes in an Amazonian floodplain lake: Santa Ninha lake. *Journal of Paleolimnology*, *48*(2), 339–350. https://doi.org/10.1007/s10933-012-9601-x

Moro, R. S., de Mattos Bicudo, C. E., de Melo, M. S., & Schmitt, J. (2004). Paleoclimate of the late pleistocene and holocene at Lagoa Dourada, Paraná state, southern Brazil. *Quaternary International*, *114*(1), 87–99. https://doi.org/10.1016/S1040-6182(03)00044-2

Nagai, R. H., Sousa, S. H. M., Burone, L., & Mahiques, M. M. (2009). Paleoproductivity changes during the Holocene in the inner shelf of Cabo Frio, southeastern Brazilian continental margin: Benthic foraminifera and sedimentological proxies. *Quaternary International*, *206*(1–2), 62–71. https://doi.org/10.1016/j.quaint.2008.10.014

Novello, V. F., Cruz, F. W., Vuille, M., Strikis, N. M., Edwards, R. L., Cheng, H., et al. (2017). A high-resolution history of the South American monsoon from last glacial maximum to the Holocene. *Scientific Reports*, *7*(1), 44267. https://doi.org/10.1038/srep44267

Nuno, P. V., Safford, H. D., & Behling, H. (2012). Holocene vegetation and fire history of the Serra do Caparaó, SE Brazil. *The Holocene*, *22*(11), 1243–1250. https://doi.org/10.1177/0959683612437864

Parizzi, M., Salgado-Labouriau, M., & Kohler, H. (1998). Genesis and environmental history of Lagoa Santa, southeastern Brazil. *The Holocene*, *8*(3), 311–321. https://doi.org/10.1191/095968398670195708

Parolin, M., Medeanic, S., & Stevaux, J. C. (2006). Registros palinologicos e mudanc¸as ambientais durante o holoceno de taquarussu (ms). *Revista Brasileira de Paleontologia*, *9*(1), 137–148. https://doi.org/10.4072/rbp.2006.1.14

Pessenda, L., Aravena, R., Melfi, A., Telles, E. C. C., Boulet, R., Valencia, E., & Filho, M. (1996). The use of carbon isotopes (^{13}C, ^{14}C) in soil to evaluate vegetation changes during the Holocene in Central Brazil. *Radiocarbon*, *38*(2), 191–201. https://doi.org/10.1017/S0033822200017562

Pessenda, L., Ribeiro, A., Gouveia, S., Aravena, R., Boulet, R., & Bendassolli, J. (2004a). Vegetation dynamics during the late Pleistocene in the Barreirinhas region, Maranhão State, northeastern Brazil, based on carbon Isotopes in soil organic matter. *Quaternary Research*, *62*(2), 183–193. https://doi.org/10.1016/j.yqres.2004.06.003

Pessenda, L. C. R., Gomes, B. M., Aravena, R., Ribeiro, A. S., Boulet, R., & Gouveia, S. E. M. (1998). The carbon isotope record in soils along a forest-Cerrado ecosystem transect: Implications for vegetation changes in the Rondonia state, southwestern Brazilian Amazon region. *The Holocene*, *8*(5), 599–603. https://doi.org/10.1191/095968398673187182

Pessenda, L. C. R., Gouveia, S. E. M., Aravena, R., Boulet, R., & Valencia, E. P. E. (2004b). Holocene fire and vegetation changes in southeastern Brazil as deduced from fossil charcoal and soil carbon isotopes. *Quaternary International*, *114*(1), 35–43. https://doi.org/10.1016/S1040-6182(03)00040-5

Pessenda, L. C. R., Gouveia, S. E. M., Ribeiro, A. D. S., De Oliveira, P. E., & Aravena, R. (2010). Late Pleistocene and Holocene vegetation changes in northeastern Brazil determined from carbon isotopes and charcoal records in soils. *Palaeogeography, Palaeoclimatology, Palaeoecology*, *297*(3–4), 597–608. https://doi.org/10.1016/j.palaeo.2010.09.008

Pessenda, L. C. R., Ledru, M. P., Gouveia, S. E. M. N., Aravena, R., Ribeiro, A. S., Bendashsollil, J. A., & Boulet, R. (2005). Holocene palaeoenvironmental reconstruction in norteastern Brazi inferred from polen, charcoal and carboon isotope records. *The Holocene*, *15*(6), 812–820. https://doi.org/10.1191/0959683605hl855ra

Pires, G., Meyer, K., & Gomes, M. (2016). Palinologia da vereda juquinha/cuba, parque estadual da serra do cabral, minas gerais, brasil. *Revista Brasileira de Paleontologia*, *19*(1), 95–110. https://doi.org/10.4072/rbp.2016.1.08

Pivel, M., Toledo, F., & Costa, K. (2010). Foraminiferal record of changes in summer monsoon precipitation at the Southeastern Brazilian continental margin since the Last Glacial Maximum. *Revista Brasileira de Paleontologia*, *13*(2), 79–88. https://doi.org/10.4072/rbp.2010.2.01

Prado, J. L., & Alberdi, M. T. (1999). The mammalian record and climatic change over the last 30,000 years in the Pampean region, Argentina. *Quaternary International*, *57–58*, 165–174. https://doi.org/10.1016/S1040-6182(98)00057-3

Prieto, A., Blasi, A., De Francesco, C., & Fernández, C. (2004). Environmental history since 11,000 14C yr B.P. of the northeastern Pampas, Argentina, from alluvial sequences of the Luján River. *Quaternary Research - QUATERNARY RES*, *62*(2), 146–161. https://doi.org/10.1016/j.yqres.2004.04.006

Raczka, M. F., De Oliveira, P. E., Bush, M., & McMichael, C. H. (2013). Two paleoecological histories spanning the period of human settlement in southeastern Brazil. *Journal of Quaternary Science*, *28*(2), 144–151. https://doi.org/10.1002/jqs.2597

Reese, C. A., Liu, K. B., & Thompson, L. G. (2013). An ice-core pollen record showing vegetation response to Late-glacial and Holocene climate changes at Nevado Sajama, Bolivia. *Annals of Glaciology*, *54*(63), 183–190. https://doi.org/10.3189/2013AoG63A375

Reißig, S., Nürnberg, D., Bahr, A., Poggemann, D.-W., & Hoffmann, J. (2019). Southward displacement of the north Atlantic subtropical gyre circulation system during north Atlantic Cold Spells. *Paleoceanography and Paleoclimatology*, *34*(5), 866–885. https://doi.org/10.1029/2018PA003376

Ribeiro, M. D. S. L., Barberi, M., & Rubin, J. (2003). ReconstruÇÃo da composiÇÃo florÍstica no decorrer dos Últimos 32.000 anos ap em Áreas de cerrados da bacia hidrogrÁfica do rio meia ponte, goiÁs, brasil. In *II Congresso sobre Planejamento e Gestão das Zonas Costeiras dos Países de Expressão Portuguesa. IX Congresso da Associa¸cão Brasileira de Estudos do Quaternário.II Congresso do Quaternário dos Países de Língua Ibéricas*.

Ruiz Pessenda, L. C., De Oliveira, P. E., Mofatto, M., de Medeiros, V. B., Francischetti Garcia, R. J., Aravena, R., et al. (2009). The evolution of a tropical rainforest/grassland mosaic in southeastern Brazil since 28,000 14C yr BP based on carbon isotopes and pollen records. *Quaternary Research*, *71*(3), 437–452. https://doi.org/10.1016/j.yqres.2009.01.008

Salgado-Labouriau, M. L., Casseti, V., Ferraz-Vicentini, K. R., Martin, L., Soubiès, F., Suguio, K., & Turcq, B. (1997). Late Quaternary vegetational and climatic changes in cerrado and palm swamp from Central Brazil. *Palaeogeography, Palaeoclimatology, Palaeoecology*, *128*(1–4), 215–226. https://doi.org/10.1016/S0031-0182(96)00018-1

Scheel-Ybert, R., Gouveia, S. E. M., Pessenda, L. C. R., Aravena, R., Coutinho, L. M., & Boulet, R. (2003). Holocene palaeoenvironmental evolution in the São Paulo State (Brazil), based on anthracology and soil $\delta^{13}C$ analysis. *The Holocene*, *13*(1), 73–81. https://doi.org/10.1191/0959683603hl596rp

Servant, M., Maley, J., Turcq, B., Absy, M.-L., Brenac, P., Fournier, M., & Ledru, M.-P. (1993). Tropical forest changes during the late quaternary in African and South American lowlands. *Global and Planetary Change*, *7*(1–3), 25–40. https://doi.org/10.1016/0921-8181(93)90038-P

Sifeddine, A., Bertrand, P., Fournier, M., Martin, L., Servant, M., Soubiès, F., et al. (1994). La sédimentation organique lacustre en milieu tropical humide (Carajas, Amazonie orientale, Brésil): Relation avec les changements climatiques au cours des 60 000 dernières années. *Bulletin de la Societe Geologique de France*, *165*, 613–621.

Sifeddine, A., Martin, L., Turcq, B., Volkmer-Ribeiro, C., Soubiès, F., Cordeiro, R. C., & Suguio, K. (2001). Variations of the Amazonian rainforest environment: A sedimentological record covering 30,000 years. *Palaeogeography, Palaeoclimatology, Palaeoecology*, *168*(3–4), 221–235. https://doi.org/10.1016/S0031-0182(00)00256-X

Sifeddine, A., Wirrmann, D., Albuquerque, A. L. S., Turcq, B., Cordeiro, R. C., Gurgel, M. H. C., & Abrão, J. J. (2004). Bulk composition of sedimentary organic matter used in palaeoenvironmental reconstructions: Examples from the tropical belt of South America and Africa. *Palaeogeography, Palaeoclimatology, Palaeoecology*, *214*(1–2), 41–53. https://doi.org/10.1016/j.palaeo.2004.06.012

Skinner, L. C., Fallon, S., Waelbroeck, C., Michel, E., & Barker, S. (2010). Ventilation of the deep Southern Ocean and deglacial CO_2 rise. *Science*, *328*(5982), 1147–1151. https://doi.org/10.1126/science.1183627

Smith, C. B., Cohen, M. C. L., Pessenda, L. C. R., França, M. C., Guimarães, J. T. F., Rossetti, D. D. F., & Lara, R. J. (2011). Holocene coastal vegetation changes at the mouth of the Amazon River. *Review of Palaeobotany and Palynology*, *168*(1), 21–30. https://doi.org/10.1016/j.revpalbo.2011.09.008

Stevaux, J. (2000). Climatic events during the late pleistocene and holocene in the upper Parana river: Correlation with NE Argentina and south-Central Brazil. *Quaternary International*, *72*(1), 73–85. https://doi.org/10.1016/S1040-6182(00)00023-9

Thompson, L. G., Mosley-Thompson, E., Davis, M. E., Lin, P.-N., Henderson, K. A., Cole-Dai, J., et al. (1995). Late glacial stage and Holocene tropical ice core records from Huascaran, Peru. *Science*, *269*(5220), 46–50. https://doi.org/10.1126/science.269.5220.46

Toledo, F. A. L., Costa, K. B., & Pivel, M. A. G. (2007). Salinity changes in the western tropical South Atlantic during the last 30 kyr. *Global and Planetary Change*, *57*(3–4), 383–395. https://doi.org/10.1016/j.gloplacha.2007.01.001

Toledo, F. A. L., Costa, K. B., Pivel, M. A. G., & Campos, E. J. D. (2008). Tracing past circulation changes in the western South Atlantic based on planktonic foraminifera. *Revista Brasileira de Paleontologia*, *11*(3), 169–178. https://doi.org/10.4072/rbp.2008.3.03

Turcq, B., Albuquerque, A. L. S., Cordeiro, R. C., Sifeddine, A., Simoes Filho, F. F. L., Souza, A. G., et al. (2002). Accumulation of organic carbon in five Brazilian lakes during the Holocene. *Sedimentary Geology*, *148*(1–2), 319–342. https://doi.org/10.1016/S0037-0738(01)00224-X

Turcq, B., Pressinotti, M. M. N., & Martin, L. (1997). Paleohydrology and paleoclimate of the past 33,000 Years at the Tamanduá river, Central Brazil. *Quaternary Research*, *47*(3), 284–294. https://doi.org/10.1006/qres.1997.1880

Vilanova, I., Prieto, A. R., & Espinosa, M. (2006). Palaeoenvironmental evolution and sea-level fluctuations along the southeastern Pampa grasslands coast of Argentina during the Holocene. *Journal of Quaternary Science*, *21*(3), 227–242. https://doi.org/10.1002/jqs.953

Wang, X., Edwards, R. L., Auler, A. S., Cheng, H., Kong, X., Wang, Y., et al. (2017). Hydroclimate changes across the Amazon lowlands over the past 45,000 years. *Nature*, *541*(7636), 204–207. https://doi.org/10.1038/nature20787

Weide, D. M., Fritz, S. C., Hastorf, C. A., Bruno, M. C., Baker, P. A., Guedron, S., & Salenbien, W. (2017). A 6000 yr diatom record of mid- to late Holocene fluctuations in the level of Lago Wiñaymarca, Lake Titicaca (Peru/Bolivia). *Quaternary Research*, *88*(2), 179–192. https://doi.org/10.1017/qua.2017.49

Weldeab, S., Schneider, R. R., & Kölling, M. (2006). Deglacial sea surface temperature and salinity increase in the western tropical Atlantic in synchrony with high latitude climate instabilities. *Earth and Planetary Science Letters*, *241*(3–4), 699–706. https://doi.org/10.1016/j.epsl.2005.11.012

Weng, C., Bush, M. B., & Athens, J. S. (2002). Holocene climate change and hydrarch succession in lowland Amazonian Ecuador. *Review of Palaeobotany and Palynology*, *120*(1–2), 73–90. https://doi.org/10.1016/S0034-6667(01)00148-8

Whitney, B., Mayle, F., Punyasena, S., Fitzpatrick, K., Burn, M., Guillen, R., et al. (2011). A 45 kyr palaeoclimate record from the lowland interior of tropical South America. *Palaeogeography, Palaeoclimatology, Palaeoecology*, *307*(1–4), 177–192. https://doi.org/10.1016/j.palaeo.2011.05.012

Zech, W., Zech, M., Zech, R., Peinemann, N., Morrás, H. J. M., Moretti, L., et al. (2009). Late Quaternary palaeosol records from subtropical (38°S) to tropical (16°S) South America and palaeoclimatic implications. *Quaternary International*, *196*(1–2), 107–120. https://doi.org/10.1016/j.quaint.2008.01.005